View Article Online
View Journal

Green Chemistry

Cutting-edge research for a greener sustainable future

Accepted Manuscript

This article can be cited before page numbers have been issued, to do this please use: F. Arfelli, N. Rivas-Márquez, H. I. M. Amin, L. Di Terlizzi, M. Fagnoni, S. Martinini, D. Ravelli, J. M. Rosas, T. Cordero, C. Samori, L. Ciacci, I. Vassura and T. Zanetta, *Green Chem.*, 2026, DOI: 10.1039/D6GC01823H.

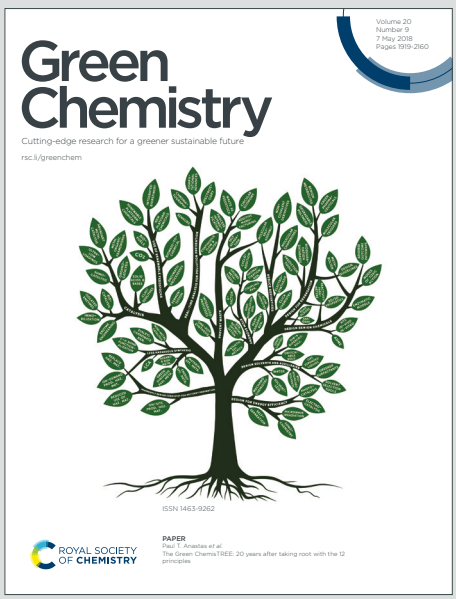

View Article Online
DOI: 10.1039/D6GC01823H

Green foundation

1. This study compares different types of photoinitiators to identify the most suitable candidate for copolymer synthesis. This preparatory phase enables the screening of promising molecules before their environmental evaluation through life cycle assessment.
2. Life Cycle Assessment is applied to the laboratory-scale synthesis of the most promising photoinitiator, where it serves as a screening tool to provide a preliminary environmental evaluation and to identify key contributors to environmental impacts.
3. A comprehensive early-stage Life Cycle Assessment has been further developed through the simulation of the industrial process. This approach would support innovative process design and enable the demonstration of potential environmental advantages at an early stage of technology development.

View Article Online
DOI: 10.1039/D6GC01823H

ARTICLE

Addressing sustainability in photopolymerization: comparative LCA study of six synthetic routes of 1-hydroxycyclohexyl phenyl ketone as photoinitiator for copolymer applications

Received 00th January 20xx,
Accepted 00th January 20xx

DOI: 10.1039/x0xx00000x

Francesco Arfelli[a*], Maria Nerea Rivas Marquez[b], Hawraz Ibrahim M. Amin[c], Lorenzo Di Terlizzi[c*], Maurizio Fagnoni[c], Samuel Martinini[a], Davide Ravelli[c], Juana Maria Rosas[b], Tomas Cordero[b], Chiara Samorì[d], Ivano Vassura[a], Tito Zanetta[e], Luca Ciacci[a,f]

Photoinitiators have long been investigated as alternatives to thermal initiators with the aim of reducing polymerisation temperatures and, consequently, heat consumption. The synthesis of poly(vinyl acetate-co-crotonic acid) represents a suitable case for exploring photoinitiation strategies. In this context, the performance of various commercial photoinitiators has been experimentally tested, and hydroxycyclohexyl phenyl ketone (HCPK) demonstrated its effectiveness with respect to other alternatives. Then, life cycle assessment (LCA) was applied to compare six alternative synthetic routes to produce HCPK, considering three different data sources: laboratory scale, advanced process calculation, and software-assisted modelling, with the latter two representative of the industrial scale. Among the six synthetic routes analysed, the pathway involving an initial α-chlorination of cyclohexyl phenyl ketone followed by a nucleophilic substitution emerges as the environmentally preferable option. As expected, a general decreasing trend in environmental impacts is observed when moving from laboratory-scale modelling to software-assisted industrial-scale modelling, likely due to process optimization at larger scales. Overall, the study demonstrates that the synthesis of poly(vinyl acetate-co-crotonic acid) is feasible through photopolymerization and that HCPK behaves better than thermal initiators like benzoyl peroxide under the same conditions. While laboratory-scale LCA constitutes a valuable preliminary screening tool, more accurate early-stage LCA modellling is likely achieved through industrial-scale simulation.

1. Introduction

Photopolymerization plays a fundamental role in various industrial applications, including 3D printing, holographic data storage, microelectronics and the preparation of adhesives and resins [1–6]. This approach has gained growing interest in recent years, mainly driven by the potential environmental benefits associated with carrying out a reaction at lower temperatures than traditional polymerization. Indeed, a twofold advantage is generally expected from the use of temperature-sensitive materials and a reduction of energy consumption [7].

Free radical polymerization of unsaturated monomers under UV or visible light irradiation is still the most popular route enabling the preparation of the desired macromolecule in a controlled manner at low temperature. The polymerization stage is promoted by the presence of a photoactive additive, behaving as a photocatalyst or, more commonly, a photoinitiator (PI) [8–13]. Type I PIs are responsible for light absorption and, in turn, undergo homolytic fragmentation upon excitation to generate a significant concentration of reactive radical intermediates in a relatively short time [14–19]. In alternative, Type II PIs may be adopted, but they require the presence of a co-initiator (a H-donor or an electron donor molecule) to promote a multi-step reaction mechanism [20].

In parallel, bio-based photopolymers are attracting increasing attention for further leveraging the sustainability of photopolymerization [21–23]. In this respect, carboxylic acid derivatives are key compounds in sustainable manufacturing, thanks to their availability in nature or easy synthesis from renewable feedstock [24–26]. In particular, many alkenoic acids, which can be obtained from natural sources, represent a promising source of bio-based monomers for renewable polyester synthesis [27–36], as demonstrated by the case of bio-based crotonic acid that can be conveniently obtained upon depolymerization of polyhydroxybutyrate (PHB) upon thermolytic distillation. The so-obtained crotonic acid shows identical physical and chemical properties compared to crotonic acid obtained from fossil resources [37], and can be used for the synthesis of poly(vinyl acetate-*co*-crotonic acid) (pCA-VA) in the presence of a thermal initiator [38].

[a.] *Department of Industrial Chemistry "Toso Montanari", University of Bologna, via Piero Gobetti 85, 40129 Bologna, Italy*
[b.] *Universidad de Málaga, Departamento de Ingeniería Química, Instituto Universitario de Materiales y Nanotecnología (IMANA), Campus de Teatinos s/n, 29071 Málaga, España.*
[c.] *PhotoGreen Lab, Department of Chemistry, University of Pavia, Viale Taramelli 12, 27100 Pavia, Italy*
[d.] *Department of Chemistry "Giacomo Ciamician", University of Bologna, Via S. Alberto 163, 48123 Ravenna, Italy.*
[e.] *R&D Vinavil SpA, Via Toce 7, 28844 Villadossola, Italy.*
[f.] *Interdepartmental Centre of Industrial Research "Renewable Resources, Environment, Sea and Energy", University of Bologna, via Angherà 22, 47922 Rimini, Italy.*

** corresponding authors*

View Article Online
DOI: 10.1039/D6GC01827H

Building on these findings, we have explored here the adoption of a photoinduced strategy for the preparation of pCA-VA in the presence of a Type I PI, in virtue of the relatively low amount of material input required for the process and the potential energy savings achievable. Due to the lack of an optimized procedure for the synthesis of pCA-VA reported in the literature [39], a small library of Type I PIs was tested to i) identify the best settings to trigger the preparation of the polymer of interest and ii) determine the environmental impact profile associated with the investigated photopolymerization, ultimately demonstrating whether the potential for environmental preferability turns into an actual impact reduction for the proposed route.

Since life cycle assessment (LCA) is the preferred methodology for environmental impact evaluation [40], we addressed the latter research question by applying LCA to the photopolymerization at the laboratory scale. More specifically, after identification of the most promising PI among those investigated, LCA was applied to compare six alternative PI synthetic routes and three different data sources covering the laboratory scale and industrial scales based on advanced process calculation and software-assisted modelling.

2. Experimental

2.1 General procedure for the photochemical synthesis of poly(vinyl acetate-co-crotonic acid)

In a flame-dried 10 mL round-bottom flask, 2 mL of freshly distilled vinyl acetate VA (ρ = 0.93 g/mL, 1.86 g; 0.01 mol), 28 mg of crotonic acid CA (1.5 wt%; bio-based or commercial origin) and 4 mL of water with polyvinyl alcohol as emulsifier (2.5 wt%) were mixed. The selected amount of the chosen photoinitiator (1-12 mg) was then added, and the round-bottom flask (25 mL) was sealed with a septum. Finally, the so-formed mixture was purged with nitrogen for 5 min and irradiated at the indicated wavelength under vigorous stirring. The polymer was obtained by precipitation in cyclohexane and subsequently dried at room temperature prior to characterization (see ESI1 for further details). The screened photoinitiators 1-hydroxycyclohexyl phenyl ketone (HCPK, commercial name: IRGACURE 184) (Fig. 1), bis(2,4,6-trimethylbenzoyl)phenylphosphine oxide (BAPO, commercial name: OMNIRAD 819), 2,2-dimethoxy-1,2-diphenylethan-1-one (DMPA) and camphorquinone (CQ) were purchased from commercial sources.

2.2 Life Cycle Assessment

LCA is a methodology standardized by ISO 14040:2006 [41] and ISO 14044:2006 [42], and it is structured into four interconnected phases: i) Goal and scope definition; ii) Life Cycle Inventory (LCI); iii) Life Cycle Impact Assessment (LCIA); and iv) Interpretation.

2.1.1 Goal and Scope definition

Since HPCK emerged as the most promising PIs, LCA is here applied to estimate and compare the environmental impacts associated with six different laboratory-scale synthesis routes for its production and three different data sources, of which one is at the laboratory scale (LAB), and two are representative of the industrial scale by means of advanced process calculation (APC) and software-assisted modelling (SAM). Specifically, to develop the up-scaled LCA model, we referred to the APC methodology defined in [43] and the ASPEN PLUS® software [44] for SAM. The three data sources provide a robust basis for discussing differences and highlighting the advantages and limitations of each approach. Finally, the contribution of the HCPK to the overall environmental impact of the final copolymer synthesis is also assessed.

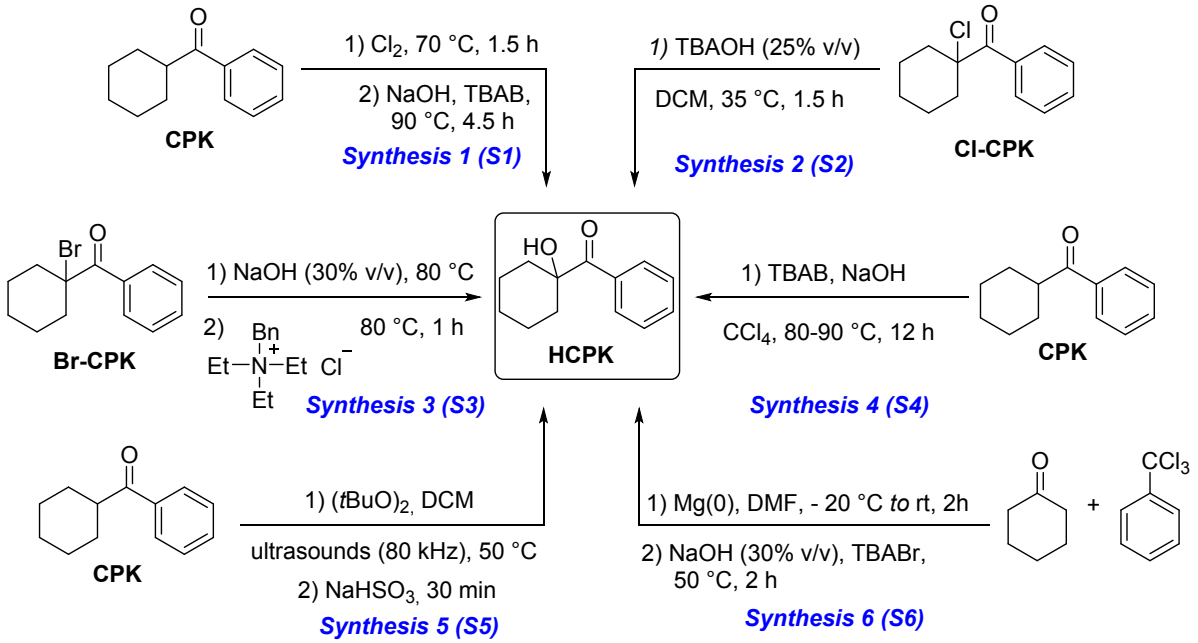

Fig. 1: Comparison of the six synthetic routes to HCPK.

The system boundaries of the models are depicted in Fig. S1 of the ESI devoted to the LCA aspects (i.e., ESI2), with gold dashed lines and include, i) extraction, production, and supply of raw materials and intermediates involved in the production; ii) generation, supply, and consumption of electricity; iii) operative phases; iv) the End-of-life (EoL) management of waste generated within the company boundaries, following a cradle-to-gate approach. The chosen system boundaries are consistent with many analyses of chemical processes [40,45,46].

The contribution of infrastructure was not included in the study, as it was considered negligible due to the relatively long service life of chemical production facilities. Although the APC framework would allow its inclusion, doing so would create an inconsistency with the Lab-scale and SAM scenarios, for which infrastructure-related contributions are not accounted for.

A literature survey was conducted, indicating six main preparation procedures [47–52]. Most of the syntheses started from cyclohexyl phenyl ketone (CPK) or the corresponding 1-bromo (Br-CPK) or 1-chloro (Cl-CPK) derivatives (Fig. 1). Results are normalized to 1 ton of product ready to be packaged and introduced in the market, identified as Functional Unit (FU). No allocation criteria were applied in the study: the environmental impacts of multifunctional processes were assigned for their total (100%) to the main product since no market-relevant by-products or co-products are generated from the synthesis. The software employed for the modelling and calculations is SimaPro 10.2.

2.1.2 Life Cycle Inventory

In this phase, the product system models are created and populated with data related to material and energy flow inventories to provide an accurate and representative system network of the processes involved in the generation of the HCPK, according to the different scenarios. In the next paragraph, the main assumptions and common aspects among the four alternatives are described.

2.1.2.1 Common assumptions

Most of the foreground processes are compiled with data reported in the synthesis described in Reaxys [53] and detailing, for instance, the amount of reactants and waste generated, and reaction yields. The six syntheses considered for comparison are described in detail in Section S1 of ESI2. Part of the foreground information has been assumed according to stoichiometry and the expertise of the authors. Each applied assumption is described and justified in the following Sections and in ESI2. Background information (e.g., inbound materials purchased by external suppliers) was drawn from the ecoinvent 3.11 database [54], the list of records used as proxies reported in Tables S1-6 of Section S1.1 in ESI2. The selected system model for the ecoinvent database records was “Cut-off”, with this being the default setting in LCA modelling.

Innovative chemical processes often involve certain reagents that are less commonly used compared to those traditionally employed in the chemical industry. The limited availability of such reagents in the relevant LCA literature is a main hindrance to comprehensive and representative estimation of a system’s environmental impacts, thereby additional modelling efforts are generally required to fill data gaps. In this view, recent literature has shown a growing interest in the Reaxys database, which contains 279 million substances and 65 million reactions. It is increasingly being used in the modelling of chemical compounds due to its extensive and detailed chemical information [55,56]. The modelling of input reagents which were not present in the available database and literature has been reported in section S1.2 of ESI2. The strategy adopted to estimate the energy consumption of each synthesis builds upon the approach described in Piccinno et al., (2016) [43] and is detailed in Section S4 of ESI2.

Concerning the management of waste originated from the syntheses (e.g., exhausted solvents, by-products), the ecoinvent record “Spent solvent mixture {Europe without Switzerland} | market for spent solvent mixture | Cut-off, U” was set as a generic reference flow in the modelling due to a lack of more substance-specific datasets. This dataset has been assigned as a proxy to each waste and byproduct that could not be directly recovered and combined with the stoichiometric composition of waste reported for each reaction for quantitative estimation of the related impacts. The process “Wastewater, unpolluted {GLO}| market for | Cut-off, U” was used for wastewater streams, assuming a low level of contamination and a high degree of dilution. For specific solvents, such as hexane, dichloromethane, dimethylformamide, and dichloroethane, a combustion stage was simulated to occur before release into the atmosphere: the resulting combustion products were included in the model (Section S2 of ESI2).

2.1.2.2 Laboratory scale

As anticipated in Section 2.2.2.1, the models related to the lab synthesis are generated according to the descriptions provided in Section 1 of ESI2. The descriptions detail the material balances, including especially the input flows (i.e., reactants, solvents) and the reaction yields. Electricity flows are measured during the process simulation by means of a Smart Meter Kekotec (operating voltage 100-250V, 50/60Hz). The electricity national mix was modelled according to the most recent available data on the International Energy Agency (IEA) website [57].

2.1.2.3 Scale Up modelling

The scale-up modelling proposed consists of two main separate frameworks, the APC and the SAM. APC adopts mathematical models to simulate chemical processes. In general, APC parametrises mass and energy balances, reaction kinetics, and thermodynamics to predict energy consumption. In this study, we built upon the framework in Piccinno et al. [43], who compiled and defined a set of equations useful for scaling chemical processes up from the Lab Scale to the industrial scale, based on physical parameters such as reactor types, mass and volume data, and estimating the energy consumption of the various

process stages. Although the work by Piccinno and colleagues constitutes a key reference in industrial chemistry modelling, their framework does not include the estimation of reaction yields or those for material recovery or recycling within the synthesis set-up boundaries. In contrast, SAM enables the virtual simulation of modelled processes, allowing the quantification of the output material flows in relation to reaction conditions. Such automation cannot be replicated through the APC, nor for laboratory-scale models. However, in the case of the APC, approximations were introduced to make the simulations more consistent with real conditions. In particular, concerning the recovery of solvents and catalysts, except for case-specific exceptions, it was assumed that 99% of the material fed into the reactors is always recovered. In all three approaches (i.e., Lab Scale, APC, and SAM), some sub-processes involved the generation of waste originate from unreacted reagents, reaction by-products and unrecovered solvents.

2.1.2.4 Advanced Process Calculation (APC)

The APC involves the use of equations to estimate the energy consumption associated with industrial processes. These equations enable estimations based on the type of reactors and mixtures used, thereby taking into account the operating conditions required to obtain the desired product at a specific yield [58]. For the case study, the accounting equations reported in Piccinno et al. [43] were applied to the processes heating, mixing, blending, grinding, filtering, distillation, vacuum drying and pumping. Specifically, the document has been adopted to estimate the energy needed for blending and heating processes. The equation reported to estimate heating energy provided by Piccinno, and colleagues takes into account the heat capacity, mass, temperature, reaction time and some dimensional parameters related to the reactor. For the more complex molecules, literature data on heat capacity were not available. To address this gap, the empirical estimation approach proposed by Xia et al. [59] was adopted, which allows the prediction of heat capacities based on molecular structure. Details of the estimations performed for the compounds involved in the syntheses are reported in Section S3 of the ESI2. One important limitation has been observed in the estimation of the heat exchange, since APC does not consider the exothermicity of reactions. For this reason, the equation reported in the document, which is reported in a simplified form in Equation 1, has been integrated by adding to the Q_{heat} (i.e., heat to supply to the reaction to be maintained at temperature T, for the time t), the reaction enthalpy, which was always lower than zero for all the synthesis, except for synthesis 5. Q_{loss} is the heat loss due to dispersion, and η_{heat} is the efficiency of the heating system. The detailed calculations are reported in Section S4 of the ESI2. In addition, the model proposed by Piccinno does not include a specific framework for modelling mass balances within reactors. To address this limitation, a set of assumptions was introduced to make the processes more realistic and consistent with an actual industrial context. For instance, gaseous reagents or inert compounds used to generate the atmosphere surrounding the reactions have been assumed to be recovered in 100%. Solvents and recoverable materials, instead, are assumed to be recycled at 99%, while the remaining 1% is assumed to be managed as waste.

Equation 1: $$Q_{react} = \frac{Q_{heat} - Q_{loss}}{\eta_{heat}} + \Delta H_r$$

2.1.2.5 Software assisted modelling (SAM)

An effective alternative for simulating a system at an industrial scale is the use of dedicated software such as ASPEN PLUS® V10 software [60]. Each synthesis of HCPK production was modelled in the ASPEN PLUS® environment, according to the flow diagrams shown in Figures S10-S15 of Section S5 in ESI2. The Non-Random Two-Liquid (NRTL) method was selected to describe the thermodynamic behaviour of the non-ideal liquid mixtures present in the organic synthesis processes analysed. The main unit operations used in the simulation were RGibbs reactors, heat exchangers (heaters/coolers) and separator blocks. The RGibbs model was selected due to the absence of kinetic information and detailed reaction mechanisms for the syntheses considered. This model determines the equilibrium composition of the reacting system by minimising the total Gibbs free energy, taking into account the conservation of the atoms of each element in the system. Thus, the composition of the output streams corresponds to the most thermodynamically stable distribution of the chemical species present. In this way, simulation allows material and energy balances to be obtained on a pilot scale, which are necessary for the design and preliminary evaluation of operational equipment.

2.3 Life Cycle Impact Assessment

The results were computed by applying the Environmental Footprint (EF) method [61] for LCIA. EF provides a comprehensive estimation of the interactions between the system under scrutiny and the environment for a set of 16 categories, namely: Acidification (AC, with mol H^+ eq as reference unit), Climate Change (CC, kg CO_2 eq), Ecotoxicity (ECOTOX, CTUe), Particulate Matter (PM, kg PM 2.5 eq), Marine Eutrophication (MEU, kg N eq), Freshwater Eutrophication (FEU, kg P eq), Terrestrial Eutrophication (TEU, kg N eq), Human carcinogenic Toxicity (HTOX_c, CTUe), Human non-carcinogenic Toxicity (HTOX_nc, CTUe), Ionizing Radiation (IR, kg U^{235} eq), Land Use (LU, Pts), Ozone Depletion (ODP, kg CFC-11 eq), Fossil Resources Depletion (FRD, MJ), Mineral Resources Depletion (kg Sb eq), Water Use (WU, m^3). The choice of the EF method was driven by the fully transparent characterization, normalization and weighting mechanisms from midpoint to endpoint results and the consistency with the spatial boundaries of the system under investigation.

2.4 Uncertainty analysis

Evaluation of uncertainty propagation in the model was performed both for midpoint and endpoint categories by employing the pedigree data quality matrix [62]. Further details about data uncertainty are reported in Table S37. Data quality

View Article Online
DOI: 10.1039/D6GC01827H

is assessed according to the derivation of the information. For all the information related to the modelled systems, geographical, temporal, and technological representativeness has been considered.

Monte Carlo simulation with 100 runs was also carried out to determine how the intrinsic variability of the parameters and the quality of the data used in the modelling affect the outcomes. The number of runs was selected by referring to Heijungs, [63] and Järviö et al. [64].

Results and Discussion

3.1 Selection of the most promising photoinitiator

The search for the best PI for the synthesis of pCA-VA copolymer implied the testing of four commercially available PIs (Fig. 2a), including colourless aryl ketones, namely DMPA and HCPK, a yellowish phosphine oxide (BAPO) [65] and a markedly yellow α-diketone (CQ) [66,67]. The UV-Vis spectra of the tested PIs are shown in Fig. 2b and allowed to select the most convenient light source to trigger the photopolymerization, including Kessil LED lamps (40 W, wavelength emission centered at 370 and 390 nm) and Evoluchem lamps (18 W, wavelength emission centered at 405 nm). The proposed screening was aimed at identifying the conditions that allowed the formation of the highest amount of polymer.

Table 1. Screening of different PIs for the polymerization of VA and CA into pCA-VA.

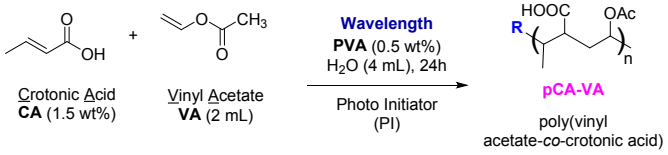

Entry	PI (amount)	Irradiation wavelength	Polymer Weight (mg)
1	DMPA (12 mg; 0.06 wt%)	390 nm	74
2	BAPO (12 mg; 0.06 wt%)	370 nm	89
3	BAPO (12 mg; 0.06 wt%)	390 nm	81
4	BAPO (12 mg; 0.06 wt%)	405 nm	185
5	CQ (12 mg; 0.06 wt%)	405 nm	40
6	HCPK (12 mg; 0.06 wt%)	370 nm	1287
7	HCPK (12 mg; 0.06 wt%)	390 nm	893
8	HCPK (12 mg; 0.06 wt%)	405 nm	1270
9	HCPK (6 mg; 0.03 wt%)	405 nm	1299
10	HCPK (3 mg; 0.016 wt%)	405 nm	1590
11	HCPK (1 mg; 0.005 wt%)	405 nm	303

Accordingly, the same amounts of monomers and additives previously used in the benzoyl peroxide-promoted thermally-initiated polymerization, were employed [38]. Thus, to a mixture containing 2 mL of vinyl acetate (VA, 1.86 g, 10 mmol), 28 mg of crotonic acid (CA, 1.5 wt%) and 10 mg (*ca*. 0.5 wt%) of polyvinylalcohol (PVA) in 4 mL of distilled water, the chosen PI was added. This mixture was then irradiated by using the less energetic light source (longer wavelength possible), overlapping with the absorption spectrum of the chosen PI.

The reaction conditions are reported in Table 1, while irradiation set-ups are shown in Fig. S1 of the Electronic Supporting Information (ESI1). The amount of polymer produced as a function of the set conditions is reported in Table 1. Fig. S2 in ESI1 depicts the polymer obtained upon irradiation of the mixture of monomers in the presence of different PIs. DMPA and CQ led to the formation of a white polymer, but in very low amounts. Similar outcomes also for BAPO at 370 and 390 nm (rows 2-3 in Table 1), while a slight increase occurred at 405 nm (185 mg). In contrast, the amount of the desired product drastically increased with HCPK as PI, with the experiment carried out at 3 mg and 0.016 wt% PI loading under irradiation at 405 nm over 24 h, performing best. Interesting to note that the amount of the polymer is markedly higher than that previously obtained by using a hazardous thermal initiator (i.e., benzoyl peroxide) upon heating [38].

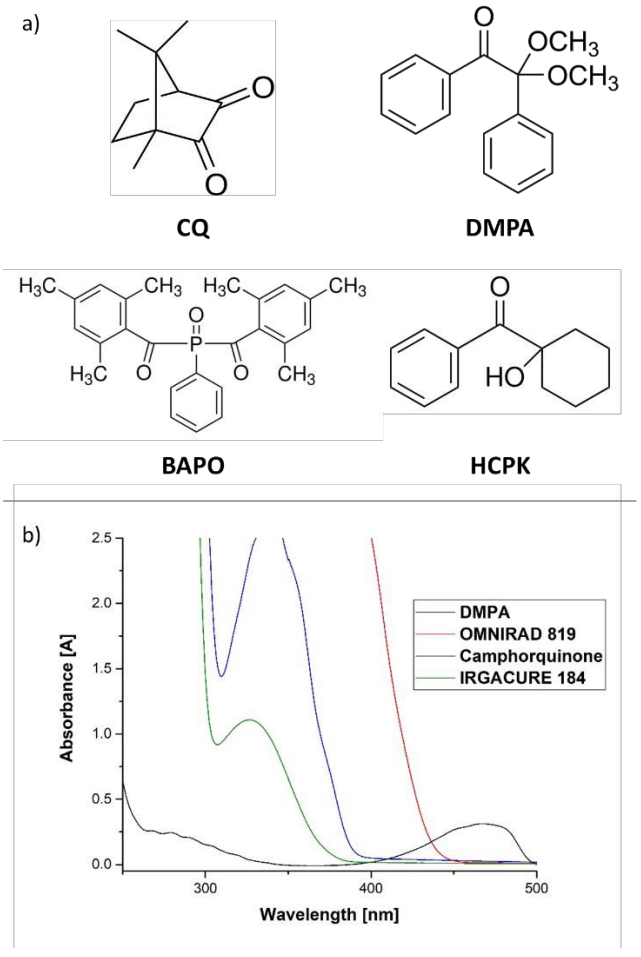

View Article Online
DOI: 10.1039/D6GC01823H

Fig. 2: a) Structure of PIs tested and b) their UV-visible spectra (10^{-2} M in MeCN).

View Article Online
DOI: 10.1039/D6GC01823H

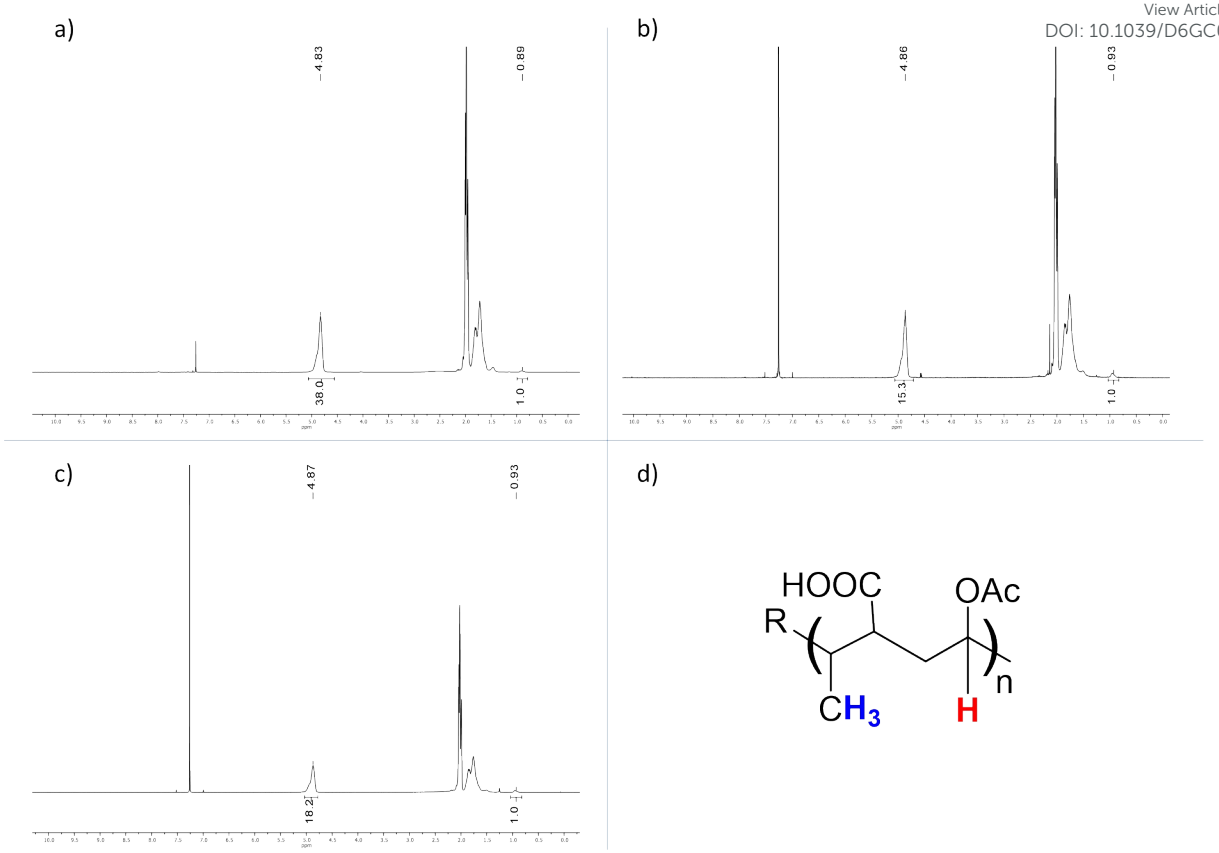

Fig. 3: a) ^{1}H-NMR analysis of the commercially available polymer; b) ^{1}H-NMR analysis of the polymer obtained from the conditions in entry 9, Table 1; c) ^{1}H-NMR analysis of the polymer obtained from the conditions in entry 10; d) pCA-VA structure.

Notably, in view of a possible industrial application, the use of a wavelength in the visible region (405 nm) is obviously desirable, due to the overall low cost of the lamps and the energy required. Moreover, since HPCK is colourless, this avoids a residual colour on the final product induced by unreactive PI or its byproducts generated by irradiation (Fig. S2 of ESI1).

Once the conditions of the polymerization process with HCPK were optimised, dedicated analyses were carried out to define the physical and chemical properties of the product obtained under those conditions. In particular, the polymers obtained in entries 9-10 of Table 1 were compared to the commercially available pCA-VA by means of both ^{1}H-NMR spectroscopy and through GPC analysis (Section S2 of ESI1). The commercial sample showed a molar ratio of CA and VA equal to 0.9: 99.1; as determined by NMR analysis (Fig. 3a). The molar ratio of the monomers incorporated in the polymer was calculated based on the ratio between the integration of the signal at ca. 0.9 ppm (blue hydrogens in Fig. 3d) and the integration of the signal at ca. 4.8 ppm (red hydrogen in Fig. 3d). The percentage of CA present in the samples derived from entries 9 and 10 was higher, with a molar ratio of 2.15 and 1.8 (Figures 3b and 3c) if compared to the commercial specimen (Fig. 3a). More details are reported in Section S3 of ESI1.
The polydispersity (PDI) of the commercially available polymer is 2.97 (Table S1 of ESI 1), while the PDI of the polymers obtained by means of the irradiation of HCPK are even lower, viz. 2.84 and 2.57, for the polymers corresponding to entries 9-10 of Table 1, respectively. The average molecular weight for the commercial sample was lower (69,373 Da) compared to those obtained in the present work (133,853 and 232,907 Da for the polymers prepared in entries 9 and 10, respectively), indicating that our samples contain longer polymeric chains with respect to the commercial one. The weight-average molecular weight, which represents the average molecular weight of a given polymer sample, was markedly higher (379,956 and 597,601 Da in the case of entries 9 and 10, respectively) than the commercial polymer (206,399 Da).
The analysis (and the amounts of polymer) obtained from entries 9 and 10 are encouraging, considering that the polymerizations were carried out under non-optimized conditions. However, the physical characterization of the resulting polymer highlights that a dedicated fine-tuning setup is required to release a commercial product suitable for sale.

3.2 Life Cycle Assessment results

Given the best performances of HCPK in the photopolymerisation of VA and CA, it was selected for a deeper investigation of the impacts associated with the replacement of traditional polymerisation with innovative ones. Thus, the potential environmental impacts associated with the six

View Article Online
DOI: 10.1039/D6GC01837H

syntheses and the three scenarios (i.e., Lab Scale, APC and SAM) described in 2.1.2 are estimated by adopting the EF 3.1 LCIA method. Complete numerical results are reported in chapter S8 of the ESI2 (Table S38-S55). Fig. 4 shows the results for CC, with details for process contributions including material inflows (i.e., reagents and solvents), energy inflows (electricity, heat, and cooling energy) and material outflows (gaseous emissions and waste). CC was selected as the reference for the graphical presentation of results. The reason for this choice is the popularity and widespread use of the category, which is also often employed as a screening indicator [68]. The other environmental categories are depicted in Fig. 5. It is specified that, in the Lab Scale scenario, electricity is used to supply all energy exchanges involved in the process, including heating and cooling. In the APC and SAM scenarios, electricity is instead consumed only for mechanical operations (e.g., mixing), while heating and cooling requirements are represented as separate energy flows. From Fig. 4, it emerges that across the scenarios, the significant role of CC is mainly associated with the supply chain of the reagents. The only exceptions occur in the Lab Scale scenario, for S3 and S6, in which solvent consumption and gaseous emissions rank as the most contributing processes, highlighting the importance of solvent and unreacted material recovery pursued at the industrial scale.

Another difference concerns the energy carriers employed: in the Lab Scale scenario, electricity is used as the only energy source, including heating. The switch from electricity to heat as an energy carrier, together with the scale-up of the equipment configuration, results in a significant potential for impact reduction. Indeed, electricity in the Lab Scale contributes between 4-39% to CC, while total energy consumed is responsible for 2-35% and 1-21% in APC and SAM scenarios, respectively. It should be noted that the energy-related impact shown in Fig. 4 refers exclusively to the energy consumed within the foreground system, while the amount of energy demanded in the background system is included in the ecoinvent proxy datasets referred to upstream material inputs, for which more complex and articulated material supply chains usually translate into higher overall environmental impacts.

Waste generation contributes to 4-36% for CC in the Lab Scale, 7-24% in the APC, and 2-24% in the SAM. High amounts of waste generated are dictated by a relatively low Atom Economy (AE). However, it is worth clarifying that the relatively higher impact contribution resulting from APC and SAM is not due to an increase in waste-related impact, but rather to the lower impact for CC estimated for these scenarios. In addition, the contribution of the EoL is also affected by the selected proxies, which are known not to be highly material-specific [69,70]. Overall, the Lab Scale scenario exhibits the highest environmental impacts, followed by the APC and SAM configurations. This outcome can be partially explained by higher energy and material use efficiency and process optimisation at full industrial scale expected in the latter scenarios. Accordingly, although the Lab Scale scenario is valuable for preliminary screening within an eco-design perspective, it cannot benchmark industrial-scale systems. Both APC and SAM scenarios revealed that the least carbon-intensive syntheses appear to be S1, S4 and S6. Considering a broader spectrum of impact categories, the descending trend switching from Lab Scale to industrial scales is confirmed. In particular, moving from Lab Scale to APC, for S4 and S6, impact values are reduced by at least 20% (up to 98.3% in S4, ODP) for all the categories.

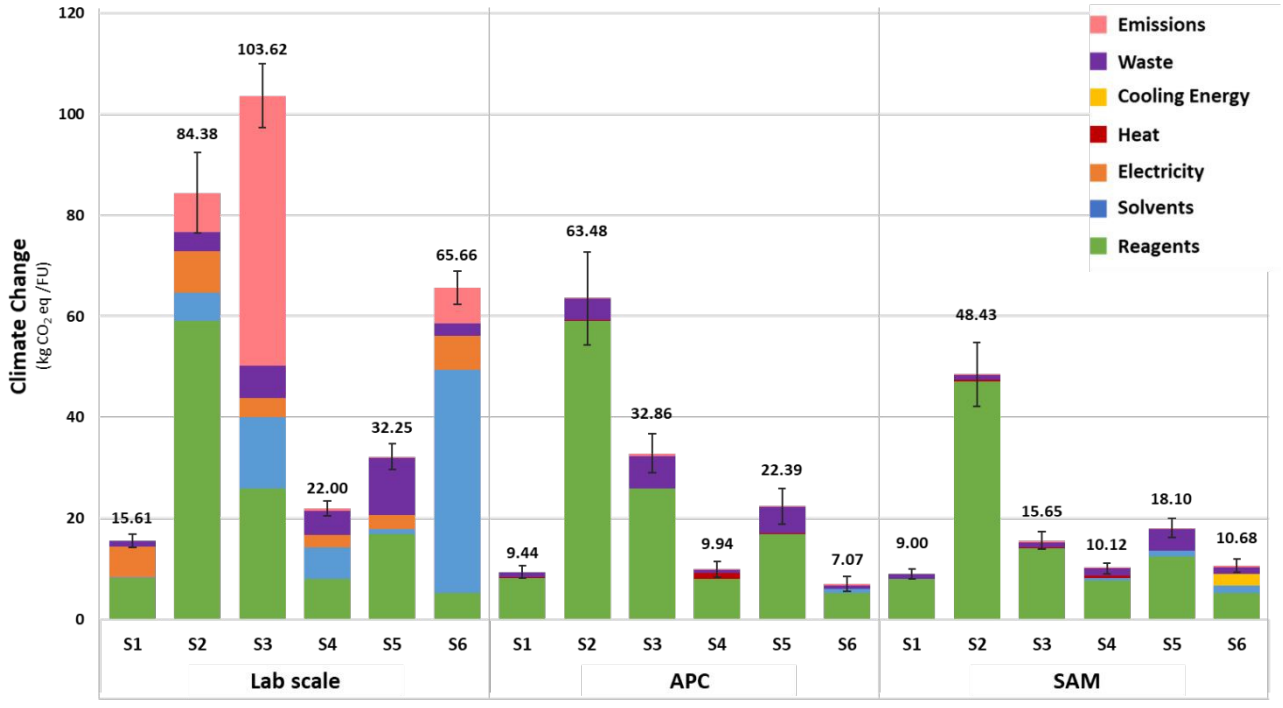

Fig. 4: Climate Change comparison between the six syntheses (S1-S6) according to the three scenarios (Lab Scale, APC, SAM).

The same for S3 and S5, with the only exception of ECOTOX, which decreased by 10.4% and 10.7%. This is due to the high contribution of the precursor (CPK or the 1-bromo derivative Br-CPK), which constitutes the main contributing element for this category, reflecting a lower implication of AE. For both S1 and S2, it is also confirmed that most impact categories show a reduction of at least 20%. Exceptions are again ECOTOX, as well as ODP, while for S2, PM makes an exception with the latter being driven by the use of TBA-OH. A similar situation occurs when switching from the Lab Scale to the SAM scenario. For S2 and S5, the impacts always decrease by more than 20%. The same for S1 and S4, with the only exception of WU in S1 and ODP (S4). In the case of S3, the 5 categories that show a decrease of less than 20% are CC, LU, POF, FRD, and WU (from 13.6% to 19.4%). Finally, for S6, the range lies between 9.8% and 27.1% for the same reason as before. In the case of S1, S2, S3, and S5, the comparison between APC and SAM indicates that the latter generally performs better. For S6, 6 out of 16 categories (AC, ECOTOX, PM, MEU, TEU, and POF) show comparatively better results under APC, while the remaining categories exhibit lower values in the SAM scenario. For S4, HTOXnc, and WU also fall into the group favouring APC. It should be noted that for S4, 13 out of 16 categories fall within a <10% difference, so the uncertainty associated with the obtained values might affect the trend resulting from nominal values. The complete outcomes of the uncertainty analysis are reported in Table S57-S73 of the ESI2. In particular, the uncertainty estimated for ECOTOX, HTOXc, HTOXncm LU and WU categories too broad to infer statistical preference between options. In the literature, it has already been highlighted that high uncertainty associated with toxicity-related categories represents a hindrance in univocal ranking of comparative studies [71,72]. Uncertainty may depend on both the inventory data quality and the selected LCIA method. However, the EF 3.1 method imported into SimaPro does not include information related to the uncertainty associated with the LCIA method. For this reason, the notable uncertainty could be justified by the standard deviation assigned to the background flows, which are not dependent on our modelling choices.

Concerning the single scenarios and starting from the Lab Scale, S2 and S6 emerge as the least environmentally favourable, each one representing the worst option for 7 out of 16 categories. For S2, this trend is also confirmed in the industrial-scale scenarios, reflecting the high contribution of input reagents, which mainly determine the environmental burdens. The reaction, in fact, exhibits a low AE: tetrabutylammonium hydroxide is introduced to replace the halogen of the CPK with a hydroxyl group, thereby generating a significant material load. Regarding S6, still at the laboratory scale, the impact contributions are largely allocated to the use of the solvent. For this reason, at the industrial scale, S6 reduces the number of categories in which it is the least favourable option from 7 to 2 (APC) and from 7 to 3 (SAM). In the case of CC, S6 represents the best option in the APC scenario.

Atmospheric emissions are the main contributor to the impacts, particularly for categories AC, PM, MEU, TEU, and POF, which are notably affected by the NO_2 emitted. CO_2 emissions also contribute, although it is more relevant at the Lab Scale due to the larger amount of waste combustion. Overall, S1 appears to be among the most promising, exhibiting the lowest impact results in 11 out of 16 categories in the Lab Scale scenario and in 10 out of 16 categories in both the APC and SAM scenarios. Although S4 ranks as the second-best synthesis route, it exhibits impact results very similar to S1, in some cases with no statistical difference in terms of expected impact. S1 and S4 are also the pathways characterized by a higher AE, since the hydroxyl group is derived from NaOH.

An aspect of interest would be to estimate the decrease in environmental impact when moving from a laboratory-scale scenario to an industrial-scale scenario. However, identifying a scaling factor, at least in this case study, is not straightforward, as the scale effect varies depending on the type of synthesis (i.e., S1–S6) and the impact category. Nevertheless, to provide some numerical insight, with the few exceptions described previously, one can reasonably expect a reduction in impact of over 20%. For the CC category, this reduction ranges from 25% to 83% in the APC scenario and from 42% to 84% in the SAM scenario. In general, it can be confirmed that APC and SAM may complement early-stage LCA estimates based on laboratory-scale data, allowing a more comprehensive perspective on the environmental profile of a product system [73,74].

We have also attempted to identify a correlation between the AE of the syntheses and the associated environmental impacts. This analysis excluded the Lab Scale scenario due to the lack of solvent recovery, which is not included in the AE calculation, as well as the related atmospheric emissions from the management of residual solvents. Regarding the APC and SAM scenarios, it appears plausible to hypothesize a relationship between AE and environmental impacts. However, some syntheses, particularly S3 and, in certain cases, S6, show deviations due to hotspots that dominate the environmental impacts, thereby altering the expected link between AE and impact. Specifically, S3 uses Br-CPK as a precursor, whose production dominates the impacts regardless of residuals and co-products formed. A similar situation is observed for S6, where the deviation is caused by nitrogen dioxide emissions (originating from the combustion of *N,N*-dimethylformamide used as a solvent). This alteration occurs in the categories most sensitive to its emissions, namely AC, MEU, TEU, and POF.

Lastly, since HCPK is used as the PI in the copolymer synthesis, assessing its contribution to the overall environmental impact of the target product would be of interest. However, such an assessment is currently not possible because no LCA studies on the synthesis of this copolymer are available in the literature, and industrial data are still considered confidential. At the current state, we can only predict that the environmental impacts associated with a relatively low mass of the PI with respect to that of the crotonic acid and vinyl acetate might be compensated by the complexity of its synthesis. Moreover, the use of HCPK should be evaluated considering the potential reduction in energy demand associated with photoinitiated polymerization.

View Article Online
DOI: 10.1039/D6GC01823H

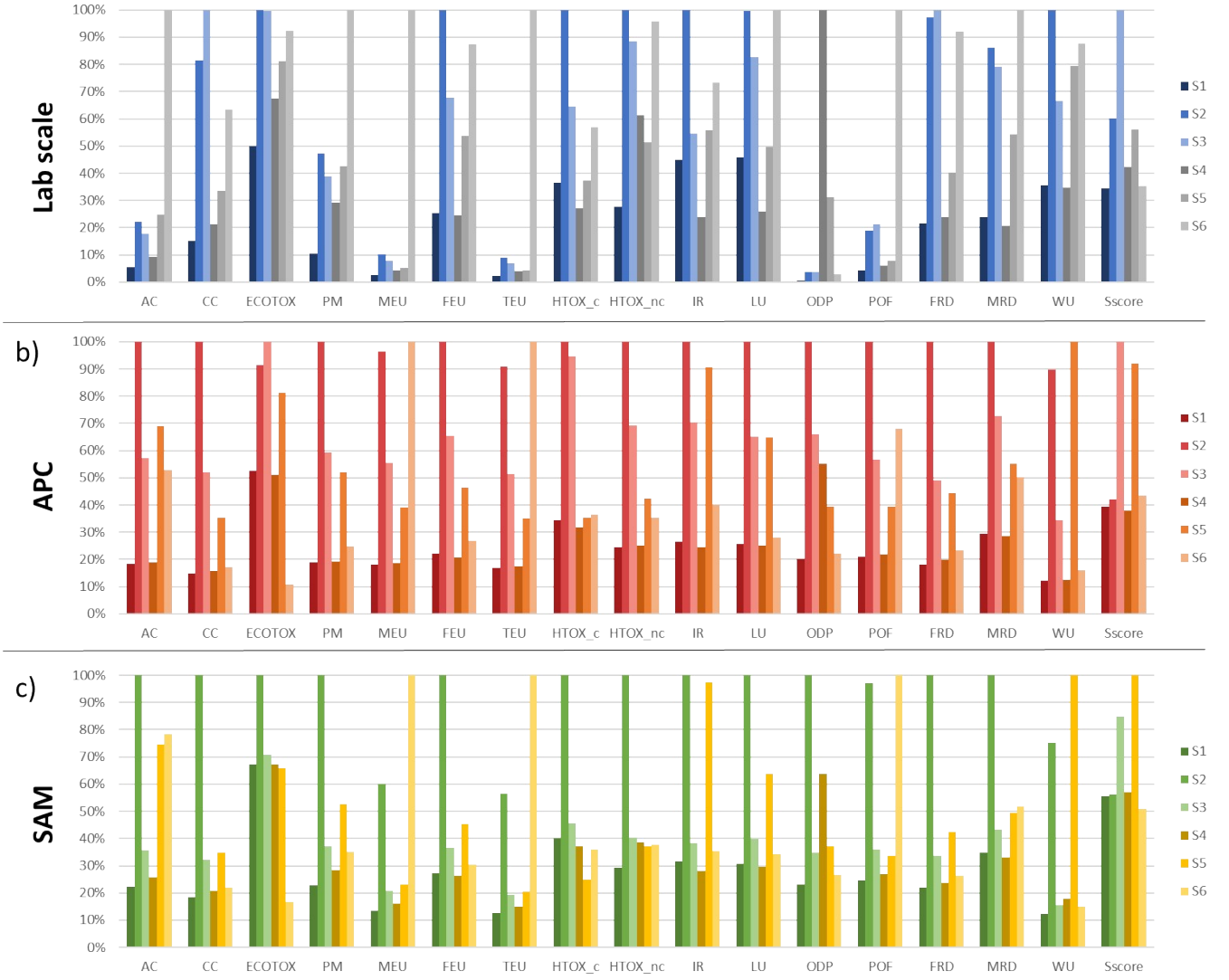

Fig. 5. Environmental impact comparison between the six syntheses (S1-S6) according to the three scenarios (Lab Scale, APC, SAM). Method EF 3.1.

Conclusions

This work demonstrated that the photopolymerisation to prepare pCA-VA may be efficiently carried out by having recourse to commercially available PIs. Among the investigated alternatives, under appropriate operating conditions, HCPK outperformed and gave the highest amount of polymer, followed by BAPO, with 10-fold worse performance. The promising results achieved with HCPK are also attractive in view of industrial implementation, as the use of wavelengths in the visible region allows for lower lamp costs and reduced energy consumption compared to the thermal alternative.

LCA methodology applied to HCPK production enabled characterization of the pros and cons of different alternative syntheses, disclosed where and why the main environmental hotspots are located in a given system, and informed about which alternative(s) should be prioritized for implementation at a larger scale, which are key elements to address sustainability in process scale-up.

APC and SAM proved to be extremely helpful in complementing early-stage LCA estimates based on data from laboratory setups, which often lack in providing a full picture of the environmental profile of a product system. From our results, in particular, SAM outcomes can likely be considered the most representative for the industrial scale. Among the six synthetic routes, the one involving an initial α-chlorination of CPK, followed by a nucleophilic substitution (S1), resulted in the most environmentally preferable. However, for some impact categories, such as FEU and HTOXc, the preferred choice remains unclear, especially when considering the results' uncertainty. While this may require accepting a trade-off between the performance of a process versus its environmental profile, it also underscores the importance of a comprehensive, broad-based perspective, such as that afforded by life-cycle

thinking approaches, to support informed choices and a continuous pursuit of improvement in the chemical industry.
Further investigation will be needed to assess the positive contribution provided by the PI, both in terms of the impacts associated with the synthesis of the PI compared to the thermal initiator, and especially in quantifying the benefits related to operating the copolymer synthesis at lower temperatures.

Author contributions

Conceptualization: FA; Data curation: FA, SM, MNRM; Formal analysis: FA, SM, MNRM, LDT, HIMA; Funding acquisition: IV, CS, MF; Investigation: LDT, HIMA; Methodology: FA, SM; Project administration: IV, CS; Resources: FA, SM, MNRM; Software: FA, MNRM; Supervision: LC, JMR, TC, MF; Validation: LC, IV; Visualization: FA, MNRM; Writing – original draft: FA, MNRM, MF, DR; Writing – review & editing: LC, IV, JMR, TC, CS, MF, DR

Conflicts of interest

There are no conflicts to declare.

Data availability

The data supporting this article have been included as part of the Supplementary Information (ESI1 and ESI2).

Acknowledgements

The authors acknowledge financial support from the European Union's Life Programme under grant agreement no. 101074164 (CROSS-LIFE – CROtonic Acid from Sewage Sludge).
This work was supported by MCIN [TED2021-131324B-C21; PID2022-140844OB-I00] and European Union "NextGenerationEU"/PRTR (MCIN/AEI/10.13039/501100011033). M.N.R.M acknowledges Junta de Andalucia/CUII and ESF+ for the award of the pre-doctoral contract (DGP_PRED_2024_01095) and the Erasmus+ Programme (KA131), the Unicaja Foundation and the University of Malaga.
Lastly, the authors also thank Giulia Borsatti (University of Pavia) for preliminary experiments.

Notes and references

1 A. Bagheri and J. Jin, *ACS Appl. Polym. Mater.*, 2019, **1**, 593–611.
2 X. He, L. Zang, Y. Xin and Y. Zou, *Applied Research*, 2023, **2**, e202300030.
3 Y. Hu, Z. Luo and Y. Bao, *Biomacromolecules*, 2025, **26**, 85–117.
4 M. Pagac, J. Hajnys, Q.-P. Ma, L. Jancar, J. Jansa, P. Stefek and J. Mesicek, *Polymers*, 2021, **13**, 598.
5 F. Petko, A. Świeży and J. Ortyl, *Polym. Chem.*, 2021, **12**, 4593–4612.
6 C. Qin, C. Sang, J. Lei, T. Xue, Z. Si and L. Wang, *Separation and Purification Technology*, 2025, **376**, 134015.
7 M. Lang, S. Hirner, F. Wiesbrock and P. Fuchs, *Polymers*, 2022, **14**, 2074.
8 M. Chen, M. Zhong and J. A. Johnson, *Chem. Rev.*, 2016, **116**, 10167–10211.
9 Y. Kwon, W. Jeon, J. Gierschner and M. S. Kwon, *Acc. Chem. Res.*, 2025, **58**, 1581–1595.
10 J. Sobieski, A. Gorczyński, A. M. Jazani, G. Yilmaz and K. Matyjaszewski, *Angew Chem Int Ed*, 2025, **64**, e202415785.
11 M. A. S. N. Weerasinghe, T. Nwoko and D. Konkolewicz, *Chem. Sci.*, 2025, **16**, 5326–5352.
12 Y. Yagci, S. Jockusch and N. J. Turro, *Macromolecules*, 2010, **43**, 6245–6260.
13 S. Zhu, W. Kong, S. Lian, A. Shen, S. P. Armes and Z. An, *Nat. Synth*, 2025, **4**, 15–30.
14 E. Dart and J. Nemcek, 1971.
15 L. Deng, L. Tang and J. Qu, *Progress in Organic Coatings*, 2020, **141**, 105546.
16 J. Fouassier and J. Lalevée, *Photoinitiators: Structures, Reactivity and Applications in Polymerization*, Wiley, 1st edn., 2021.
17 J. Klee, M. Maier and C. Fik, DOI:10.1002/9781119006671.fmatter.
18 S. M. Müller, S. Schlögl, T. Wiesner, M. Haas and T. Griesser, *ChemPhotoChem*, 2022, **6**, e202200091.
19 Y. Zhang, Y. Xu, A. Simon-Masseron and J. Lalevée, *Chem. Soc. Rev.*, 2021, **50**, 3824–3841.
20 J. P. Fouassier and J. Lalevée, *Photoinitiators for Polymer Synthesis: Scope, Reactivity and Efficiency*, Wiley, 1st edn., 2012.
21 I. Chiulan, E. B. Heggset, Ş. I. Voicu and G. Chinga-Carrasco, *Biomacromolecules*, 2021, **22**, 1795–1814.
22 R. Hu, J. Zhan, Y. Zhao, X. Xu, G. Luo, J. Fan, J. H. Clark and S. Zhang, *Green Chem.*, 2023, **25**, 8970–9000.
23 F. Sacchi, G. Colucci, F. Bondioli, M. Sangermano and M. Messori, *J Mater Sci*, 2025, **60**, 11191–11220.
24 I. Hevus, N. G. Ricapito, S. Tymoshenko, S. N. Raja and D. C. Webster, *ACS Sustainable Chem. Eng.*, 2020, **8**, 5750–5762.
25 V. Kumar, P. Kumar, S. K. Maity, D. Agrawal, V. Narisetty, S. Jacob, G. Kumar, S. K. Bhatia, D. Kumar and V. Vivekanand, *Biotechnol Biofuels*, 2024, **17**, 72.
26 N. Teramoto, M. Ozeki, I. Fujiwara and M. Shibata, *J of Applied Polymer Sci*, 2005, **95**, 1473–1480.
27 R. Bafana and R. A. Pandey, *Critical Reviews in Biotechnology*, 2018, **38**, 68–82.
28 J. G. H. Hermens, A. Jensma and B. L. Feringa, *Angew Chem Int Ed*, 2022, **61**, e202112618.
29 J. Lebeau, J. P. Efromson and M. D. Lynch, *Front. Bioeng. Biotechnol.*, 2020, **8**, 207.
30 G. B. Pedroso, S. Montipó, D. A. N. Mario, S. H. Alves and A. F. Martins, *Biomass Conv. Bioref.*, 2017, **7**, 23–35.
31 C. A. Roa Engel, A. J. J. Straathof, T. W. Zijlmans, W. M. Van Gulik and L. A. M. Van Der Wielen, *Appl Microbiol Biotechnol*, 2008, **78**, 379–389.
32 B.-E. Teleky and D. Vodnar, *Polymers*, 2019, **11**, 1035.
33 Y. Wu, M. Shetty, K. Zhang and P. J. Dauenhauer, *ACS Eng. Au*, 2022, **2**, 92–102.
34 S. Yang, M. Kim, S. Yang, D. S. Kim, W. J. Lee and H. Lee, *Catal. Sci. Technol.*, 2016, **6**, 3616–3622.
35 T. Yang, W. Li, Q. Liu, M. Su, T. Zhang and J. Ma, *BioRes*, 2019, **14**, 5025–5044.
36 K. Yang, L. Zhu, Y. Zhao, Z. Wei, X. Chen, C. Yao, Q. Meng and R. Zhao, *Bioresource Technology*, 2019, **293**, 122095.
37 A. Parodi, A. Jorea, M. Fagnoni, D. Ravelli, C. Samorì, C. Torri and P. Galletti, *Green Chem.*, 2021, **23**, 3420–3427.

38 A. Jorea, A. Parodi, T. Benelli, L. Ciacci, M. Fagnoni, P. Galletti, L. Mazzocchetti, D. Ravelli, C. Torri, I. Vassura and C. Samorì, *RSC Sustainability*, 2023, **1**, 1035–1042.
39 D. Donescu and L. Fusulan, *Journal of Dispersion Science and Technology*, 1996, **17**, 631–644.
40 F. Arfelli, D. Maria Pizzone, D. Cespi, L. Ciacci, R. Ciriminna, P. Salvatore Calabrò, M. Pagliaro, F. Mauriello and F. Passarini, *Waste Management*, 2023, **168**, 156–166.
41 ISO 14040:2006/Amd 1:2020 Environmental management — Life cycle assessment — Principles and framework
42 ISO 14044:2006/Amd 2:2020 Environmental management — Life cycle assessment — Requirements and guidelines
43 F. Piccinno, R. Hischier, S. Seeger and C. Som, *Journal of Cleaner Production*, 2016, **135**, 1085–1097.
44 AspenTech, 2026. https://www.aspentech.com/en/products/engineering/aspen-plus
45 M. A. F. Delgove, A. Laurent, J. M. Woodley, S. M. A. De Wildeman, K. V. Bernaerts and Y. van der Meer, *ChemSusChem*, 2019, **12**, 1349–1360.
46 S. V. Mankar, M. N. Garcia Gonzalez, N. Warlin, N. G. Valsange, N. Rehnberg, S. Lundmark, P. Jannasch and B. Zhang, *ACS Sustainable Chem. Eng.*, 2019, **7**, 19090–19103.
47 D. Zhou, CN102267887A, 2011.
48 R. Wu, Q. Zhang, M. Xiang, Guihong and J. Zhang, CN109503343B, 2018.
49 E. Meneguzzo, G. Norcini and G. Li Bassi, WO2009135895A1, 2008.
50 Q. Chen and Q. Huang, CN108911959A, 2018.
51 F. Wang, CN109694310A, 2018.
52 J. Sun, CN109896942A, 2017.
53 Elsevier, 2026. https://www.reaxys.com/
54 G. Wernet, C. Bauer, B. Steubing, J. Reinhard, E. Moreno-Ruiz and B. Weidema, *Int J Life Cycle Assess*, 2016, **21**, 1218–1230.
55 L. Berti, F. Arfelli, F. Villa, F. Cappitelli, D. Gulotta, L. Ciacci, E. Bernardi, I. Vassura, F. Passarini, S. Napoli and S. Goidanich, *Heritage*, 2024, **7**, 6871–6890.
56 D. Cespi, *Green Chem.*, 2024, **26**, 9554–9568.
57 IEA, 2026. https://www.iea.org/countries/italy/electricity
58 Pushpendra, A. Schonhoff, S. C. Füchsl, H. Röder and P. Zapp, *Journal of Cleaner Production*, 2025, **498**, 145208.
59 L. Xia, Y. Pan, T. Zhao, X. Sun, S. Tao, Y. Chen and S. Xiang, *Chinese Journal of Chemical Engineering*, 2023, **57**, 30–38.
60 X.-Q. Tan, W. Mo, A. R. Mohamed and W.-J. Ong, *Journal of Cleaner Production*, 2024, **436**, 140270.
61 European Commission, European Platform on LCA | EPLCA, https://eplca.jrc.ec.europa.eu/, (accessed March 10, 2026).
62 B. P. Weidema and M. S. Wesnæs, *Journal of Cleaner Production*, 1996, **4**, 167–174.
63 R. Heijungs, *Probability, Statistics and Life Cycle Assessment: Guidance for Dealing with Uncertainty and Sensitivity*, Springer International Publishing, Cham, 2024.
64 N. Järviö, T. Parviainen, N.-L. Maljanen, Y. Kobayashi, L. Kujanpää, D. Ercili-Cura, C. P. Landowski, T. Ryynänen, E. Nordlund and H. L. Tuomisto, *Nat Food*, 2021, **2**, 1005–1013.
65 J. E. Baxter, R. S. Davidson, H. J. Hageman, L. A. McLauchlan and D. G. Stevens, *J. Chem. Soc., Chem. Commun.*, 1987, 73–75.
66 M. Mitterbauer, M. Haas, H. Stüger, N. Moszner and R. Liska, *Macro Materials & Eng*, 2017, **302**, 1600536.
67 N. Moszner, F. Zeuner, I. Lamparth and U. K. Fischer, *Macro Materials & Eng*, 2009, **294**, 877–886.
68 M. Z. Hauschild, R. K. Rosenbaum and S. I. Olsen, 2018.
69 F. Arfelli, M. Roguszewska, G. Torta, M. Iurlo, D. Cespi, L. Ciacci and F. Passarini, *Sustainable Production and Consumption*, 2024, **49**, 318–328.
70 M. Haupt, T. Kägi and S. Hellweg, *Data in Brief*, 2018, **19**, 1441–1457.
71 Y. Chen, S. Li and R. Kang, *Reliability Engineering & System Safety*, 2021, **215**, 107896.
72 E. Rossi, F. Arfelli, L. Barani, D. Cespi, L. Ciacci and F. Passarini, *Science of The Total Environment*, 2024, **955**, 177289.
73 N. R. D. De Souza, L. Matt, R. Sedrik, L. Vares and F. Cherubini, *Sustainable Production and Consumption*, 2023, **43**, 319–332.
74 H. Minten, B. D. Vandegehuchte, B. Jaumard, R. Meys, C. Reinert and A. Bardow, *Green Chem.*, 2024, **26**, 8728–8743.

View Article Online
DOI: 10.1039/D6GC01823H

View Article Online
DOI: 10.1039/D6GC01823H

Data availability

The data supporting this article have been included as part of the Supplementary Information (ESI1 and ESI2).